Published OnlineFirst April 21, 2016; DOI: 10.1158/2159-8290.CD-16-0075

RESEARCH BRIEF

EGFR Fusions as Novel Therapeutic Targets in Lung Cancer

Kartik Konduri[1,2], Jean-Nicolas Gallant[3], Young Kwang Chae[4,5,6], Francis J. Giles[4,5,6], Barbara J. Gitlitz[7,8], Kyle Gowen[9], Eiki Ichihara[10], Taofeek K. Owonikoko[11,12], Vijay Peddareddigari[13,14], Suresh S. Ramalingam[11,12], Satyanarayan K. Reddy[11,12], Beth Eaby-Sandy[13], Tiziana Vavalà[8,15], Andrew Whiteley[1], Heidi Chen[16], Yingjun Yan[10], Jonathan H. Sheehan[17,18], Jens Meiler[18,19], Deborah Morosini[9], Jeffrey S. Ross[9,20], Philip J. Stephens[9], Vincent A. Miller[9], Siraj M. Ali[9], and Christine M. Lovly[3,8,10,21]

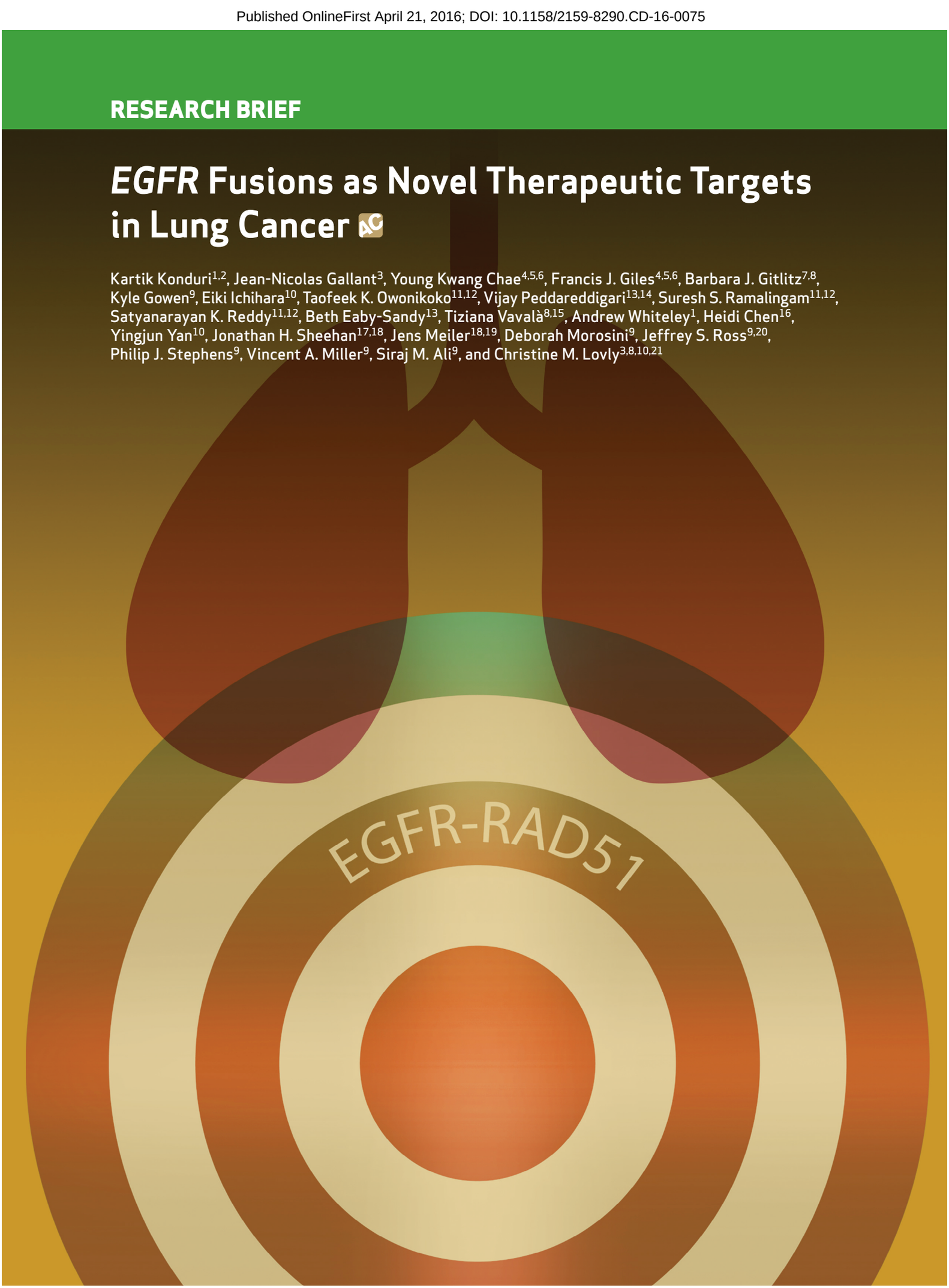

Published OnlineFirst April 21, 2016; DOI: 10.1158/2159-8290.CD-16-0075

ABSTRACT Here, we report that novel epidermal growth factor receptor (*EGFR*) gene fusions comprising the N-terminal of EGFR linked to various fusion partners, most commonly RAD51, are recurrent in lung cancer. We describe five patients with metastatic lung cancer whose tumors harbored *EGFR* fusions, four of whom were treated with EGFR tyrosine kinase inhibitors (TKI) with documented antitumor responses. *In vitro*, EGFR–RAD51 fusions are oncogenic and can be therapeutically targeted with available EGFR TKIs and therapeutic antibodies. These results support the dependence of *EGFR*-rearranged tumors on EGFR-mediated signaling and suggest several therapeutic strategies for patients whose tumors harbor this novel alteration.

SIGNIFICANCE: We report for the first time the identification and therapeutic targeting of EGFR C-terminal fusions in patients with lung cancer and document responses to the EGFR inhibitor erlotinib in 4 patients whose tumors harbored *EGFR* fusions. Findings from these studies will be immediately translatable to the clinic, as there are already several approved EGFR inhibitors. *Cancer Discov; 6(6); 601–11. ©2016 AACR.*

See related commentary by Paik, p. 574.

INTRODUCTION

Oncogenic mutations in the epidermal growth factor receptor (EGFR) are found in a subset of patients with non–small cell lung cancer (NSCLC) and serve as important predictive biomarkers in this disease (1–3). These mutations, which most commonly occur as either small in-frame deletions in exon 19 or point mutations in exon 21 (L858R) within the EGFR tyrosine kinase domain, confer constitutive activity and sensitivity to EGFR tyrosine kinase inhibitors (TKI). Several large phase III clinical trials have shown that patients with *EGFR*-mutant lung cancer derive superior clinical responses when treated with EGFR TKIs as compared with standard chemotherapy (4–6), and several EGFR inhibitors are already FDA approved. These trials used PCR-based "hotspot" testing, which typically interrogates for *EGFR* point mutations and small indels in exons 18 to 21. More recently, next-generation sequencing (NGS) of tumor samples has allowed for the identification of additional mechanisms whereby the EGF receptor may become aberrantly activated (7, 8), further documenting the importance of EGFR signaling in the pathogenesis of lung cancer. Here we report, for the first time in lung cancer, the presence of oncogenic *EGFR* fusions, most commonly *EGFR–RAD51*, which contain the entire EGFR tyrosine kinase domain fused to RAD51, a protein involved in DNA-damage responses. We demonstrate that these fusions are oncogenic in preclinical studies and show that patients whose tumors harbor *EGFR* fusions derive significant clinical benefit from treatment with EGFR TKI therapy.

RESULTS

Frequency of *EGFR* Alterations in Lung Cancer

To determine the frequency of *EGFR* fusions in lung cancer, we analyzed data from ~10,000 clinical cases (Supplementary Table S1). Fusion events, defined by a genomic breakpoint in *EGFR* exons 23 through intron 25, were detected in 5 patients, each of which is described below.

Case Reports

Patient 1, a 35-year-old woman, was diagnosed with metastatic lung adenocarcinoma after presenting with generalized weakness and worsening vision. Imaging studies revealed widespread disease in the bone, liver, lymph nodes, adrenal glands, and hard palate (Table 1). MRI showed innumerable metastases in the brain, dura, and left globe, resulting in retinal detachment. She was initially treated with radiotherapy to the brain and spine. Due to significant debility in the setting of tumor-induced disseminated intravascular coagulation (DIC), she was a poor candidate for cytotoxic chemotherapy.

[1]Baylor University Medical Center, Baylor Sammons Cancer Center, Dallas, Texas. [2]Texas Oncology PA, Dallas, Texas. [3]Department of Cancer Biology, Vanderbilt University Medical Center, Nashville, Tennessee. [4]Northwestern Medicine Developmental Therapeutics Institute, Chicago, Illinois. [5]Robert H. Lurie Comprehensive Cancer Center of Northwestern University, Chicago, Illinois. [6]Northwestern University Feinberg School of Medicine, Chicago, Illinois. [7]Department of Medicine, University of Southern California Keck School of Medicine, Los Angeles, California. [8]Addario Lung Cancer Medical Institute, Cambridge, Massachusetts. [9]Foundation Medicine, Inc., Cambridge, Massachusetts. [10]Department of Medicine, Vanderbilt University Medical Center, Nashville, Tennessee. [11]Department of Hematology and Medical Oncology, Emory University School of Medicine, Atlanta, Georgia. [12]Winship Cancer Institute, Atlanta, Georgia. [13]Abramson Cancer Center, Hospital of the University of Pennsylvania, Philadelphia, Pennsylvania. [14]Janssen Research & Development, LLC, Horsham, Pennsylvania. [15]Department of Oncology, Thoracic Oncology Unit, University of Turin, Italy. [16]Department of Biostatistics, Vanderbilt University Medical Center, Nashville, Tennessee. [17]Department of Biochemistry, Vanderbilt University Medical Center, Nashville, Tennessee. [18]Center for Structural Biology, Vanderbilt University Medical Center, Nashville, Tennessee. [19]Department of Chemistry, Vanderbilt University Medical Center, Nashville, Tennessee. [20]Albany Medical College, Albany, New York. [21]Vanderbilt-Ingram Cancer Center, Vanderbilt University Medical Center, Nashville, Tennessee.

Note: Supplementary data for this article are available at Cancer Discovery Online (http://cancerdiscovery.aacrjournals.org/).

K. Konduri, J.-N. Gallant, Y.K. Chae, F.J. Giles, B.J. Gitlitz, K. Gowen, E. Ichihara, T.K. Owonikoko, V. Peddareddigari, S.S. Ramalingam, S.K. Reddy, B. Eaby-Sandy, T. Vavalà, and A. Whiteley contributed equally to this article.

Corresponding Author: Christine M. Lovly, Vanderbilt-Ingram Cancer Center, 2220 Pierce Avenue South, 777 Preston Research Building, Nashville, TN 37232-6307. Phone: 615-936-3457; Fax: 615-343-2973; E-mail: christine.lovly@vanderbilt.edu

doi: 10.1158/2159-8290.CD-16-0075

Published OnlineFirst April 21, 2016; DOI: 10.1158/2159-8290.CD-16-0075

Table 1. Clinical characteristics of patients with NSCLC harboring *EGFR* kinase fusions

Patient no.	Age	Gender	Ethnicity	Diagnosis	Smoking status	Sites of disease	Prior treatment	*EGFR* fusion	EGFR TKI	Best response	Duration of EGFR TKI therapy
1	35	Female	South Asian	Stage IV lung adenocarcinoma	Never	Lung Lymph nodes Bone Brain Adrenal gland Breast Peritoneum Eye	- RT to the whole brain and T8 vertebra	*EGFR-RAD51*	Erlotinib	PR	8 months
2	21	Female	Caucasian	Stage IV lung adenocarcinoma	3 pack years	Lung Lymph nodes Bone Brain	- RT to the thoracic spine - Radiosurgery to brain mets - RT to the right hip	*EGFR-RAD51*	Erlotinib	PR	5 months
3	43	Female	Caucasian	Stage IV lung adenocarcinoma	10 pack years, quit > 10 years ago	Lung Bone Brain	- WBI - Carboplatin, pemetrexed, bevacizumab, 6 cycles	*EGFR-PURB*	Erlotinib	PR	20 months, ongoing
4	38	Male	Caucasian	Stage IV lung adenocarcinoma	Former light smoker (3 pack years)	Lung Lymph nodes Pleura Bone	- Cisplatin/ pemetrexed, 6 cycles - Maintenance pemetrexed, 11 cycles	*EGFR-RAD51*	Erlotinib	PR	6 months, ongoing
5	60	Female	Caucasian	Stage IV lung adenocarcinoma	Never	Lung Lymph nodes Brain	- Craniotomy - RT to surgical bed - Carboplatin/ pemetrexed, 4 cycles - Maintenance pemetrexed, 6 cycles	*EGFR-RAD51*	N/A	N/A	N/A

Abbreviations: RT, radiation therapy; WBI, whole-brain irradiation; PR, partial response; N/A, not applicable; Mets, metastases.

Published OnlineFirst April 21, 2016; DOI: 10.1158/2159-8290.CD-16-0075

A lymph-node biopsy was sent for genomic profiling using an extensively validated hybrid capture–based NGS diagnostic platform (FoundationOne; ref. 9) and found to harbor a novel *EGFR* rearrangement at exon 25, resulting in the formation of an *EGFR–RAD51* fusion gene (Fig. 1A and B; Supplementary Table S2). The patient was treated with the EGFR TKI erlotinib. Within 2 weeks of erlotinib initiation, the DIC had resolved (Supplementary Fig. S1A), and the patient experienced clinical improvement with a noticeable decrease in supraclavicular lymphadenopathy and a hard palate metastatic lesion. After 6 months of treatment, the primary left lung mass and largest two liver lesions had decreased by 69% per RECIST (10; Fig. 1C; Supplementary Fig. S1B), and the patient experienced an improvement in her functional status. She remained on erlotinib for 8 months, after which she experienced disease progression.

Patient 2, a 21-year-old woman, was diagnosed with metastatic lung adenocarcinoma after presenting with right shoulder pain and unintentional weight loss. MRI revealed extensive metastatic disease in the spine and a right paraspinal mass extending into neuroforamina. Additional imaging studies showed metastatic disease in the brain, innumerable lung nodules, lymph nodes, and right acetabulum. Biopsy of an axillary lymph node showed metastatic adenocarcinoma consistent with lung primary. NGS testing revealed an *EGFR–RAD51* fusion. The patient received palliative radiotherapy to the spine and brain metastases. Subsequently, the patient reported hemoptysis and dyspnea with exertion. Complete blood count showed a marked drop in platelet number and elevated lactate dehydrogenase, consistent with DIC. She was not a candidate for systemic chemotherapy. She was started on erlotinib approximately 6 weeks after initial presentation. Thrombocytopenia resolved within 10 days (Supplementary Fig. S2A), and the patient experienced symptomatic improvement. CT scans obtained 3 months after the initiation of erlotinib showed a significant regression of bilateral miliary nodules as well as a 43% decrease in the index lesions of the left lower lobe (LLL), subcarinal lymph node, and right apical soft-tissue mass compared with baseline (Fig. 1C; Supplementary Fig. S2B). The patient remained on erlotinib for 5 months with response, but she is no longer taking this medication due to nonmedical issues.

Patient 3, a 42-year-old woman, was diagnosed with metastatic lung adenocarcinoma after presenting with right hip pain. Imaging studies revealed widespread disease, including the primary left lower lobe (LLL) lesion, lytic lesions in the right pelvis and acetabulum, and brain metastases. Biopsy of a lung mass was positive for adenocarcinoma. She was initially treated with whole-brain radiotherapy and platinum-based chemotherapy with a partial response. While receiving chemotherapy, her tumor biopsy sample was sent for NGS testing and found to harbor an *EGFR* rearrangement at exon 25, resulting in the formation of a fusion gene between *EGFR* and *PURB* (Supplementary Table S2; Supplementary Fig. S3A and S3B). At the time of disease progression on chemotherapy, the patient was treated with erlotinib, resulting in a 48% decrease in the LLL index lesion, ongoing for 20 months (Fig. 1C; Supplementary Fig. S3C).

Patient 4, a 38-year-old man, was diagnosed with metastatic lung adenocarcinoma after presenting with dyspnea and progressive weakness. Imaging studies showed metastatic disease to the lungs, lymph nodes, pleura, and bone. A pleural biopsy was performed, and NGS testing identified an *EGFR–RAD51* fusion. He was initially treated with cisplatin/pemetrexed followed by maintenance pemetrexed. At the time of disease progression, the patient was started on erlotinib, with partial response after two cycles of therapy (Fig. 1C; Supplementary Fig. S4). The patient has now received erlotinib for 6 months with continued response.

Patient 5, a 60-year-old woman, initially presented with headache, slurred speech, and left foot drag. MRI revealed three enhancing cerebral masses with midline shift. Further imaging studies showed a 4-cm mass in the lingula and lymphadenopathy. Biopsy of the lung mass revealed adenocarcinoma. The patient underwent resection of a right frontal tumor followed by radiotherapy. She was treated with four cycles of carboplatin/pemetrexed with partial response, followed by pemetrexed maintenance therapy. During this treatment, NGS testing was completed and revealed an *EGFR–RAD51* fusion. The patient continues to receive benefit from pemetrexed therapy; she has not yet been treated with an EGFR TKI.

EGFR–RAD51 Is Oncogenic

We stably expressed EGFR variants in Ba/F3 cells and detected expression of EGFR–RAD51 at the expected molecular weight as compared with EGFR wild-type (WT) and the known oncogenic $EGFR^{L858R}$ mutation (Fig. 2A). We observed that, analogous to $EGFR^{L858R}$, EGFR–RAD51 was able to activate downstream signaling through the MAPK and PI3K/AKT pathways. EGFR–RAD51 was also able to sustain IL3-independent proliferation of Ba/F3 cells, an activity phenotype associated with the transforming function of other oncogenic tyrosine kinases (Fig. 2B; ref. 11). In parallel, we expressed the same EGFR variants in NR6 cells (which lack endogenous EGFR; ref. 12; Supplementary Fig. S5A and S5B). EGFR–RAD51 significantly increased colony formation of NR6 cells in soft agar—a hallmark of tumor cells—as compared with control cells and those expressing $EGFR^{WT}$ (Supplementary Fig. S5C and S5D).

EGFR contains several autophosphorylation sites in the C-terminal tail of the receptor (including tyrosines 992, 1068, and 1173) that positively regulate the transforming activity of EGFR by mediating downstream proliferative signaling (13). These autophosphorylation sites, which serve as docking sites for signaling adaptor proteins, are lacking in the EGFR–RAD51 fusion (Figs. 1B and 2C). Notably, however, EGFR–RAD51 contains tyrosine 845, a phosphorylation site within the kinase domain that is critical for complete EGFR function and transformation in NSCLC (14). The presence of tyrosine 845 may explain why EGFR–RAD51 is still able to activate downstream oncogenic signaling via the PI3K/AKT and MAPK pathways (Fig. 2A and C). Notably, these EGFR fusions also lack tyrosine 1045, the CBL binding site that targets EGFR for degradation. Indeed, EGFR–RAD51 is more stable (has a slower turnover rate) compared with $EGFR^{WT}$ (Supplementary Fig. S6A and S6B), suggesting that EGFR–RAD51 receptor stability might also play a role in its oncogenic properties. Taken together, these data support that EGFR–RAD51 is able to activate tumorigenic signaling and confer an oncogenic phenotype.

Published OnlineFirst April 21, 2016; DOI: 10.1158/2159-8290.CD-16-0075

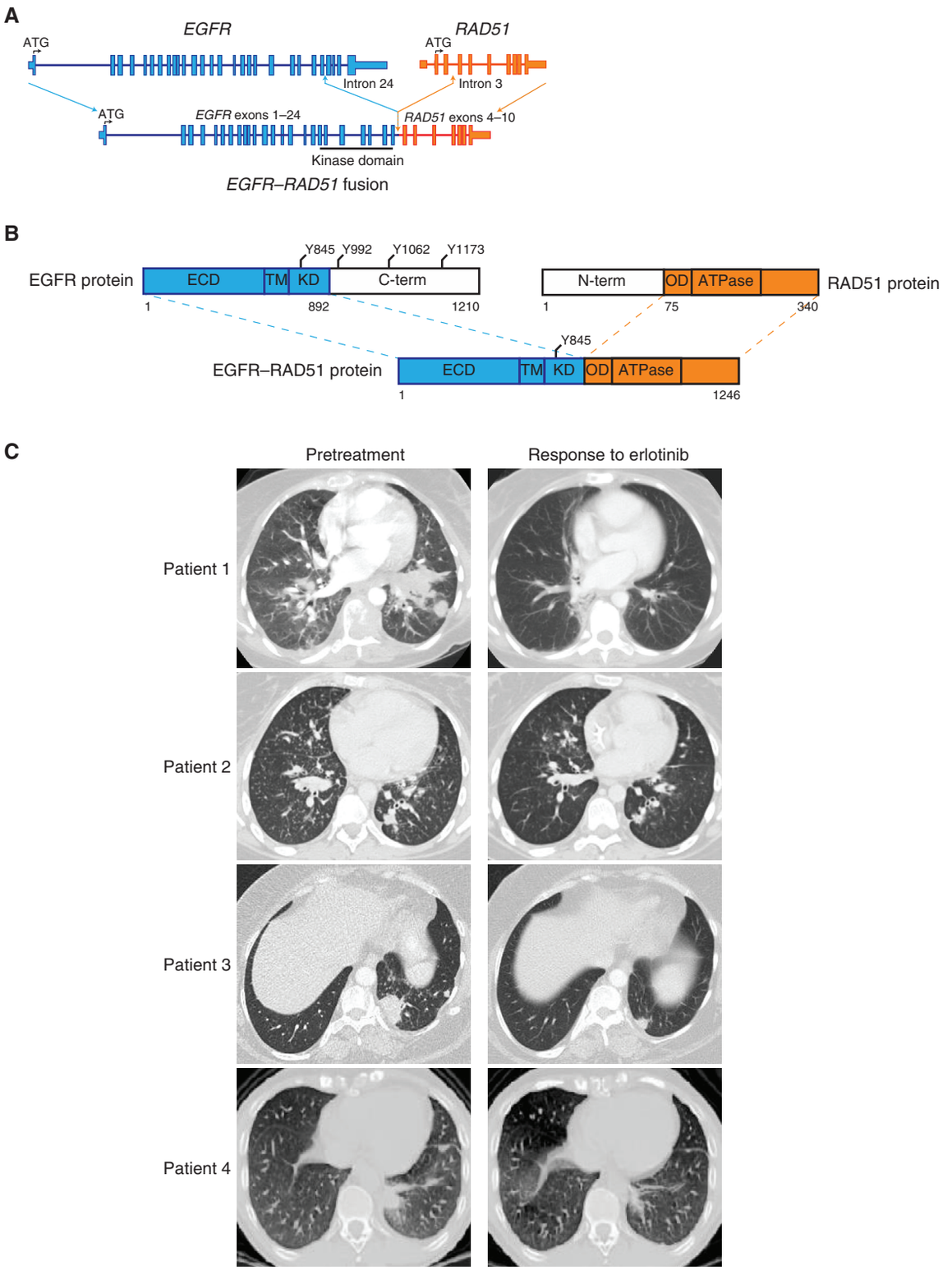

Figure 1. EGFR fusions are clinically actionable. **A,** scaled representation of *EGFR–RAD51* depicting the genomic structure of the fusion. ATG, translational start site; blue, *EGFR*; orange, *RAD51*. **B,** schematic representation of the EGFR–RAD51 fusion protein domain structure. Numbers correspond to amino acid residues. Y, tyrosine residue; ECD, extracellular domain; TM, transmembrane domain; KD, kinase domain; C-term, carboxyl terminus; N-term, amino terminus; OD, oligomerization domain/section; ATPase, adenylpyrophosphatase; blue, EGFR; orange, RAD51. **C,** serial CT scans from index patients with lung adenocarcinoma harboring *EGFR* fusions, documenting response to the EGFR TKI erlotinib. Left images, scans obtained prior to initiation of erlotinib. Right images, scans obtained during erlotinib therapy.

Published OnlineFirst April 21, 2016; DOI: 10.1158/2159-8290.CD-16-0075

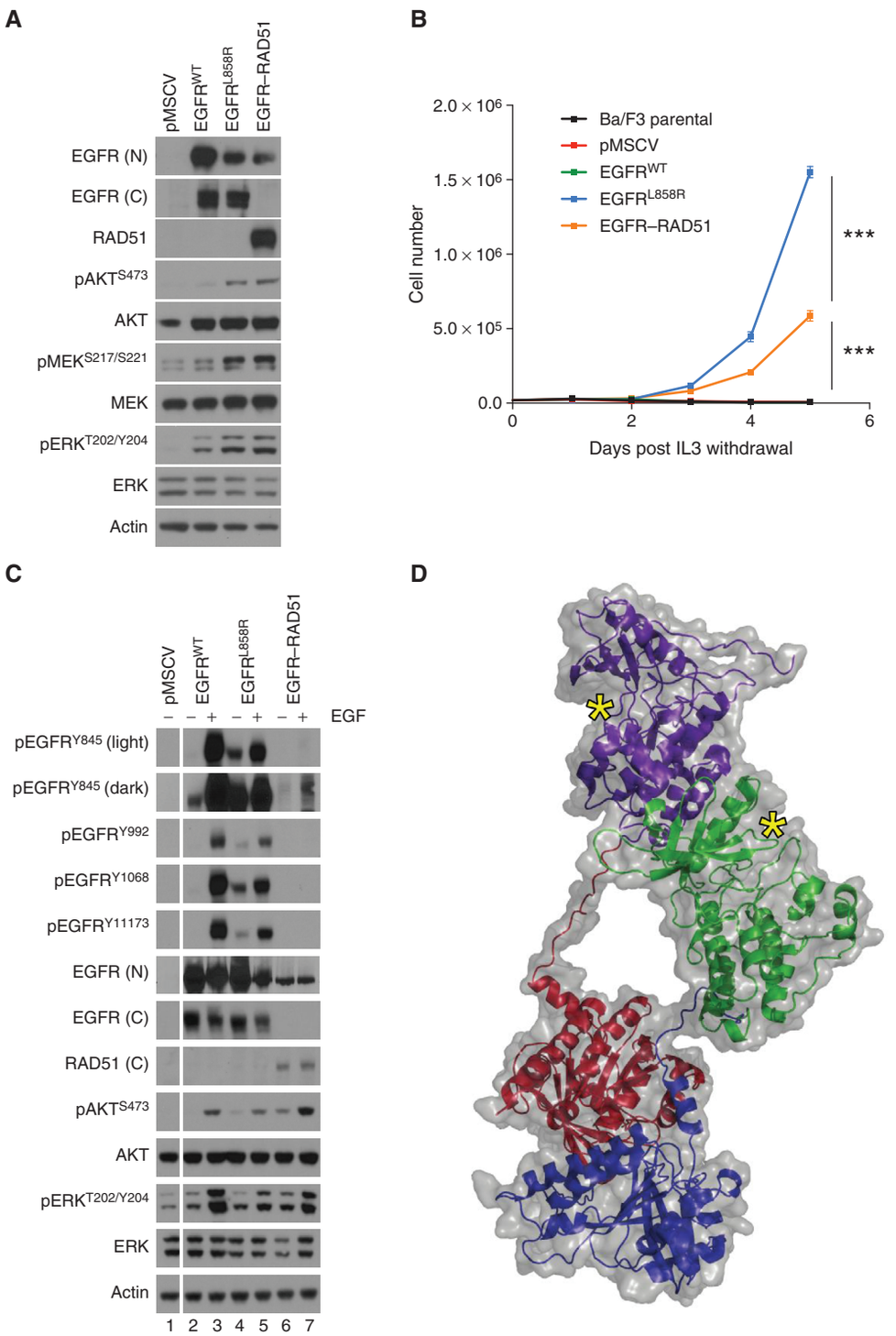

Figure 2. EGFR–RAD51 is an oncogenic *EGFR* alteration. **A,** Ba/F3 lines stably expressing pMSCV (vector only), $EGFR^{WT}$, $EGFR^{L858R}$ or EGFR–RAD51 were subjected to Western blot analysis with indicated antibodies. The three distinct EGFR variants were detected at the anticipated molecular weight (MW) of ~150 kD. EGFR–RAD51 fusion is detected with both the N-terminal EGFR antibody [EGFR(N)] and with the RAD51 antibody. There is no cross-reactivity between wild-type RAD51 protein, which has an MW of ~35 kD, and the EGFR–RAD51 fusion. **B,** Ba/F3 cells transfected with indicated constructs (pMSCV, vector only) were grown in the absence of IL3 and counted every 24 hours. ***, $P < 0.0001$. **C,** Ba/F3-expressing EGFR variants were serum starved for 16 hours, treated with 50 ng/mL EGF for 5 minutes, and subjected to Western blot analysis with indicated antibodies. **D,** ribbon diagram and space-filling model of the EGFR–RAD51 kinase domains illustrating the proposed mechanism of activation. Purple, first EGFR kinase domain; green, second EGFR kinase domain; red, first RAD51 partner; blue, second RAD51 partner; yellow asterisks, active sites.

Published OnlineFirst April 21, 2016; DOI: 10.1158/2159-8290.CD-16-0075

Computational Modeling of EGFR–RAD51

The EGFR tyrosine kinase is activated through ligand-mediated formation of asymmetric (N-lobe to C-lobe) dimers (15). Kinase fusions, on the other hand, commonly share a mechanism of activation whereby the fusion partner drives dimerization of the kinase and leads to ligand-independent activation (16). Given the presence of RAD51, a self-assembling filamentous protein (17), we hypothesized that the EGFR–RAD51 fusion protein can form such partner-driven dimers. To validate this hypothesis, we modeled EGFR–RAD51 based on available experimental structures of RAD51 and the active asymmetric EGFR dimer. Conformational loop sampling with Rosetta demonstrates that it is geometrically feasible for EGFR kinase subunits to adopt the asymmetric (active) dimeric conformation when fused to RAD51 (Fig. 2D). Further, the concatenation of RAD51 subunits could bring tethered EGFR kinase domains close together, increasing their local concentration and leading to further EGFR activation (Supplementary Fig. S7). Although this structural modeling demonstrates that the EGFR–RAD51 is geometrically capable of forming active dimers, further experimental data are needed to confirm this mechanism.

EGFR–RAD51 Can Be Therapeutically Targeted with Existing EGFR Inhibitors

The finding of recurrent *EGFR* fusions in lung cancer is of particular interest because EGFR TKIs have proven an effective therapeutic strategy for tumors harboring certain *EGFR* mutations. Therefore, we sought to determine the effectiveness of EGFR TKIs against EGFR–RAD51. We treated Ba/F3 cells expressing EGFR–RAD51 with erlotinib (first-generation reversible EGFR TKI), afatinib (second-generation irreversible EGFR/HER2 TKI), and osimertinib (third-generation irreversible EGFR TKI) to assess the effects of these inhibitors on cellular proliferation. $EGFR^{L858R}$ served as a positive control in this experiment. Each TKI effectively inhibited the growth of Ba/F3 cells expressing EGFR–RAD51 to varying degrees (Fig. 3A; Supplementary Table S3). Downstream MAPK and PI3K/AKT signaling was also inhibited with TKI treatment (Fig. 3B). The on-target effect of EGFR TKIs could be observed when blotting for phosphotyrosine from immunoprecipitated EGFR–RAD51 protein (Fig. 3C) and when observing the phosphorylation status of tyrosine 845, which is included in the fusion protein (Supplementary Fig. S8). Finally, we tested the effects of the FDA-approved EGFR antibody cetuximab in our cell culture models. Cetuximab binds to the EGFR extracellular domain and blocks the binding of growth factors, such as EGF (18). In contrast to $EGFR^{L858R}$, proliferation of Ba/F3 cells expressing EGFR–RAD51 was potently inhibited by cetuximab (Fig. 3D and E; Supplementary Fig. S9). Together, these results show that EGFR–RAD51 can be potently inhibited by a variety of EGFR-targeted agents, suggesting several intriguing clinical avenues.

DISCUSSION

Just over 10 years ago, "canonical" EGFR point mutations and short indels in the kinase domain were detected retrospectively by PCR-based "hotspot" testing in patients with lung cancer who responded to EGFR TKI therapy (1–3). Assessing for these "canonical" EGFR mutations is now the accepted standard of care worldwide for patients with lung cancer. Here, by utilizing a comprehensive NGS assay that interrogates the entire coding region of *EGFR* (as well as introns 7, 15, 24, 25, and 26), we identified novel *EGFR* fusions in patients with lung cancer—*EGFR–RAD51* and *EGFR–PURB*—that would otherwise have gone undetected by the standard of care.

Although distinct *EGFR* fusions have previously been observed in glioma (19), this is the first documentation of patients with *EGFR* fusion–positive tumors that derived significant and sustained antitumor responses from treatment with the EGFR TKI erlotinib. Our *in vitro* work also hints at afatinib being potent against EGFR–RAD51—highlighting that the structural effects of the EGFR mutation, the resultant conformation of the EGFR kinase domain, and the type of EGFR inhibitor are all important factors in determining the efficacy of a specific EGFR TKI against a particular EGFR mutation (20).

Interestingly, EGFR–RAD51 fusions were markedly sensitive to both EGFR TKIs and the EGFR antibody cetuximab. Although some unselected patients with NSCLC respond to cetuximab, the monoclonal anti-EGFR antibody adds minimal benefit for most patients—even when combined with chemotherapy (21, 22). Previous work has shown that cetuximab sensitivity is correlated with asymmetric dimerization (23). As our modeling suggests that the EGFR–RAD51 fusion is activated by virtue of constitutive dimerization, these findings suggest a unique molecular cohort that may benefit from cetuximab. Further, these findings provide a rationale for therapeutically targeting this subset of lung cancers with a wide array of anti-EGFR therapies, many of which are already FDA approved. Ongoing work will elucidate whether the deregulated RAD51 component of the EGFR–RAD51 fusion protein may also be a therapeutic vulnerability for treatment with platinum-based and PARP-inhibitor therapies.

Our experimental work also demonstrates that EGFR–RAD51 fusions are oncogenic and able to mediate downstream signaling through the MAPK and PI3K/AKT pathways. Although this may seem surprising, given that EGFR–RAD51 fusions lack the C-terminal tail known to be important for EGFR signal transduction, analyses of several cancer types have identified EGFR C-terminal deletions as recurrent and transforming events (24–26). The exact mechanism whereby these EGFR C-terminal deletions activate the EGFR kinase domain and confer transforming properties remains unclear. In the case of EGFR–RAD51 fusions, we believe there is a unique role for RAD51 given the specific fusion event's recurrence. A common characteristic of tyrosine kinase fusions is that the fusion partner (here, RAD51) contributes an oligomerization domain, which promotes activation of the kinase (27). As demonstrated by our structural modeling, EGFR–RAD51 fusion proteins could be activated by virtue of RAD51 oligomerization. Similarly, structural modeling has shown that PURB proteins can self-associate in the absence of nucleic acids (28). Additional experimental work will be required to determine whether activation of EGFR fusion proteins is driven by asymmetric dimerization of the EGFR tyrosine kinase domain, dimerization through the known partner oligomerization interface, or both.

Published OnlineFirst April 21, 2016; DOI: 10.1158/2159-8290.CD-16-0075

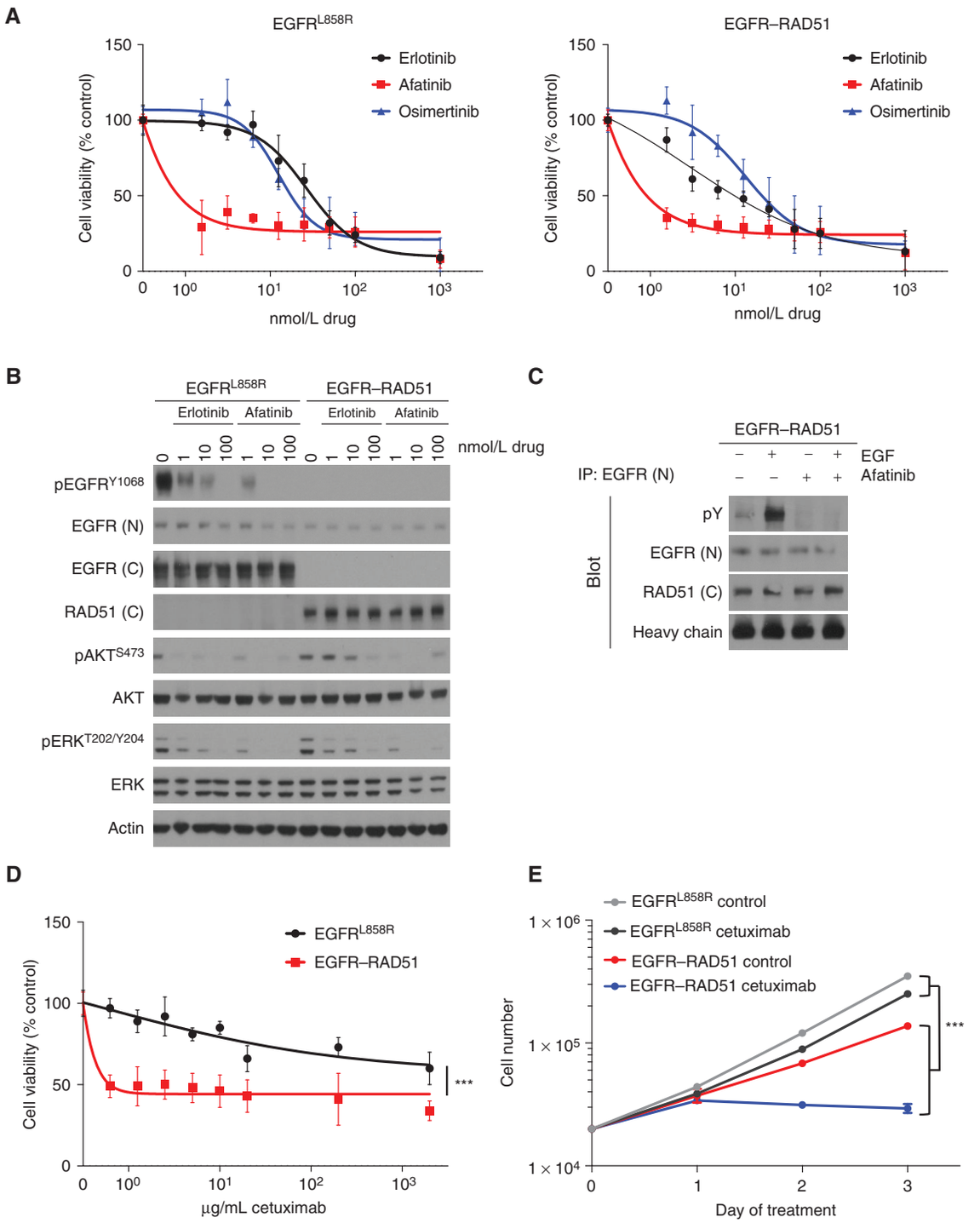

Figure 3. EGFR-RAD51 is therapeutically targetable with EGFR inhibitors. **A,** Ba/F3 lines stably expressing EGFR^{L858R} or EGFR-RAD51 were treated with increasing doses of erlotinib, afatinib, or osimertinib for 72 hours. CellTiter-Blue assays were performed to assess cell viability. Each point represents six replicates. Data are presented as the mean percentage of viable cells compared with vehicle control ± SD. **B,** Ba/F3 lines stably expressing EGFR^{L858R} or EGFR-RAD51 were treated with increasing doses of erlotinib or afatinib for 2 hours and subjected to Western blot analysis with indicated antibodies. **C,** Ba/F3 cells stably expressing EGFR-RAD51 were serum starved for 16 hours and then treated with 100 nmol/L afatinib for 1 hour followed by 50 ng/mL EGF for 5 minutes. EGFR was immunoprecipitated from cellular lysates with an antibody targeting the EGFR N-terminus and then subjected to Western blot analysis with indicated antibodies. **D,** Ba/F3 cells stably expressing EGFR^{L858R} or EGFR-RAD51 were treated with increasing doses of cetuximab for 72 hours. CellTiter-Blue assays were performed to assess cell viability. Each point represents six replicates. Data are presented as the mean percentage of viable cells compared with vehicle control ± SD. ***, $P < 0.0001$. **E,** Ba/F3 cells stably expressing EGFR^{L858R} or EGFR-RAD51 were treated with 5 μg/mL cetuximab and counted every 24 hours. Each point represents the average of three replicates ± SD. ***, $P < 0.0001$.

Published OnlineFirst April 21, 2016; DOI: 10.1158/2159-8290.CD-16-0075

The cases presented here highlight that adjusting our strategy and using newly available tools, such as comprehensive NGS tests, could prove useful in detecting alternative ways in which the EGFR pathway is altered (and can be targeted) in tumors. Based on the observation that the *EGFR–RAD51* fusions detected in the first two patients occurred with breakpoints in *EGFR* intron 24, we defined further fusion events by the presence of a genomic breakpoint in *EGFR* exons 23 through intron 25. Although we limited our investigation to these parameters, we cannot exclude that other *EGFR* rearrangements may exist in lung cancer outside of these parameters. Refinements in the assay may enable the discovery of more clinically relevant *EGFR* fusions or alterations in the future.

METHODS

Cell Culture

Ba/F3 cells were purchased from DSMZ. Plat-GP cells were purchased from CellBioLabs. NR6 cells have been previously described (12). Ba/F3 cells were maintained in RPMI-1640 medium (Mediatech, Inc.). NR6 and Plat-GP cells were maintained in DMEM (Gibco). Media were supplemented with 10% heat-inactivated fetal bovine serum (Atlanta Biologicals) and penicillin–streptomycin (Mediatech, Inc.) to final concentrations of 100 U/mL and 100 μg/mL, respectively. The Ba/F3 cell line was supplemented with 1 ng/mL murine IL3 (Gibco). The Plat-GP cell line was cultured in the presence of 10 μg/mL blasticidin (Gibco). All cell lines were maintained in a humidified incubator with 5% CO_2 at 37°C and routinely evaluated for *Mycoplasma* contamination. Besides verifying the status of *EGFR* mutations in cell lines, no additional cell line identification was performed.

In Vitro *Analysis of the EGFR–RAD51 Fusion Protein*

Plasmids containing *EGFR–RAD51* were constructed based on the reported genomic sequence (Supplementary Fig. S10). NR6 and Ba/F3 cells were transduced with retrovirus encoding *EGFR* variants. Functional analyses, including colony formation, proliferation, and response to EGFR inhibitors, were performed as previously described (7).

Immunoprecipitation and Immunoblotting

For immunoprecipitation, cells were harvested, washed in PBS, and lysed in non-denaturing lysis buffer (1% Triton-X-100, 137 mmol/L NaCl, 10% glycerol, 20 mmol/L Tris–HCl, pH 8.0) with freshly added 40 mmol/L NaF, 1 mmol/L Na-orthovanadate, and protease inhibitor mini tablets (Thermo Scientific). Protein was quantified using protein assay reagent and a SmartSpec plus spectrophotometer (Bio-Rad) per the manufacturer's protocol. Lysates (300–500 μg) were subjected to overnight immunoprecipitation with 2 μg N-term EGFR clone 528 (Santa Cruz#120; 10 μL). Antibody was precipitated with Protein A Dynabeads (Invitrogen). Immunoblotting was then performed as described below. Please see the Supplementary Methods for details of all of the antibodies used in this study.

For immunoblotting, cells were harvested, washed in PBS, and lysed in RIPA buffer (150 mmol/L NaCl, 1% Triton-X-100, 0.5% Na-deoxycholate, 0.1% SDS, 50 mmol/L Tris–HCl, pH 8.0) with freshly added 40 mmol/L NaF, 1 mmol/L Na-orthovanadate, and protease inhibitor mini tablets (Thermo Scientific). Protein was quantified (as detailed above) and 20 μg of lysates were subjected to SDS-PAGE. Protein was transferred to PVDF membranes (Millipore) at 1,000 mA·h, blocked in 5% BSA, and incubated with antibodies as detailed above. Detection was performed using Western Lightning ECL reagent (Perkin Elmer) and autoradiography film paper (Denville). Samples analyzed with N-term EGFR clone 528 were prepared under nonreducing and nonboiled conditions.

Cell Viability, Counting, and Clonogenic Assays

For viability experiments, cells were seeded at 5,000 cells/well in 96-well plates and exposed to treatment the following day. At 72 hours after drug addition, Cell Titer Blue reagent (Promega) was added, and fluorescence at 570 nm was measured on a Synergy MX microplate reader (BioTek) according to the manufacturer's instructions. For cell counting experiments, cells were seeded at 10,000 cells/well in 24-well plates in the absence of 1 ng/mL IL3. Every 24 hours, cells were diluted 20-fold and counted using a Z1 Coulter Counter (Danaher). For cell counting experiments with drug, cells were seeded at 20,000 cells/well in 12-well plates in the absence of 1 ng/mL IL3. Drugs were added at the following concentrations: erlotinib 500 nmol/L, afatinib 50 nmol/L, osimertinib 500 nmol/L, and cetuximab 5 μg/mL. Every 24 hours, cells were diluted 20-fold and counted using a Z1 Coulter Counter (Danaher). Viability assays were set up in sextuplicate, clonogenic assays were set up in triplicate, and cell-counting assays were set up in triplicate. All experiments were performed at least three independent times. Data are presented as the percentage of viable cells compared with control (vehicle-only treated) cells. To determine the IC_{50} values, regressions were generated as asymmetric sigmoidal dose–response curves using Prism 6 (GraphPad).

Structural Modeling of the EGFR–RAD51 Fusion

The sequence of the EGFR–RAD51 fusion protein was used to generate a structural model based on the crystal structure templates 1SZP.PDB (*S. cerevisiae* RAD51; ref. 17) and 2GS6.PDB (human EGFR; ref. 15). PyMOL version 1.5.0.3 (Schrödinger) was used to combine two monomers of yeast RAD51 and two kinase domains of EGFR into a single template structure for input to modeling. The N-termini of the RAD51 domains were positioned close to the C-termini of the EGFR domains to represent the fusion result. Modeller version 9.14 (29) was then used to generate the dimeric model of the fusion protein structure. The conformational space for the dimer was then sampled using Rosetta version 2015.05 (30). A total of 20,000 independent modeling runs were performed using kinematic loop closure. To illustrate the arrangement of the filament, the crystallographic symmetry records from 1SZP.PDB were then used to construct eight additional copies of the complex in PyMOL.

Clinical Data and Tumor Genotyping

All patient data were acquired under Institutional Review Board (IRB)–approved protocols. Informed consent was obtained from all patients. Samples were deidentified, protected health information reviewed according to the Health Insurance Portability and Accountability Act (HIPAA) guidelines, and studies conducted in accordance with the Declaration of Helsinki. Genomic profiling of tumor samples was performed using a hybrid capture–based NGS diagnostic platform (FoundationOne; ref. 9).

Identification of EGFR Genomic Alterations in Lung Cancer Diagnostic Specimens

The database of >56,000 Foundation Medicine clinical cases (Primary_150929_114735; November 2, 2015) was interrogated for rearrangement class events to identify those cases likely to harbor an *EGFR* fusion event using the FoundationOne Molecular Information Browser v0.8. Cases involving an event with a genomic breakpoint in *EGFR* exons 23 through intron 25 were manually investigated to evaluate the potential of each individual rearrangement. Exon boundaries were chosen based on the index cases (*EGFR–RAD51* harboring a genomic breakpoint in *EGFR* intron 24).

Published OnlineFirst April 21, 2016; DOI: 10.1158/2159-8290.CD-16-0075

Statistical Analysis and Data Presentation

All experiments were performed using at least three technical replicates and at least two independent times (biological replicates). For statistical analyses, all biological and technical replicates were pooled to perform an integrated assessment on the differences among groups. To determine the differences in cell counts, time, and dose trends, and in order to account for the dependence of technical replications and repeated measurements, the linear mixed model was used to perform the analysis. The assumption of normality for the mixed model was investigated. If necessary, data were transformed using log transformation for the linear mixed model. R3.2.2 (www.R-project.org) was used to perform all statistical analyses.

Each figure or panel shows a single representative experiment with the statistical significance derived from integrated experimental analyses—as described above. Unless indicated otherwise, data are presented as mean ± standard deviation. Western blot autoradiography films were scanned in full color at 600 dpi, desaturated in Adobe Photoshop CC, and cropped in Powerpoint. Genomic and proteomic diagrams were created in Adobe Illustrator CC. Patient images were cropped to highlight the region of interest. No other image alterations were made.

Disclosure of Potential Conflicts of Interest

K. Konduri is a consultant/advisory board member for Boehringer Ingelheim. B.J. Gitlitz has received speakers bureau honoraria from Genentech. K. Gowen has ownership interest (including patents) in FMI. S.S. Ramalingam is a consultant/advisory board member for Genentech, AstraZeneca, Lilly, Boehringer Ingelheim, Novartis, BMS, and Merck. B. Eaby-Sandy has received speakers bureau honoraria from Amgen, Celgene, Merck, and Eisai, and is a consultant/advisory board member for Clovis and AstraZeneca. J.S. Ross reports receiving a commercial research grant from Foundation Medicine and has ownership interest (including patents) in the same. P.J. Stephens has ownership interest (including patents) in Foundation Medicine. V.A. Miller has ownership interest (including patents) in Foundation Medicine. S.M. Ali has ownership interest (including patents) in Foundation Medicine. C.M. Lovly reports receiving commercial research grants from AstraZeneca, Novartis, and Xcovery; has received speakers bureau honoraria from Qiagen; and is a consultant/advisory board member for Pfizer, Novartis, Sequenom, Ariad, Clovis, and Genoptix. No potential conflicts of interest were disclosed by the other authors.

Authors' Contributions

Conception and design: K. Konduri, J.-N. Gallant, Y.K. Chae, F.J. Giles, T.K. Owonikoko, S.S. Ramalingam, J. Meiler, J.S. Ross, S.M. Ali, C.M. Lovly

Development of methodology: J.-N. Gallant, F.J. Giles, J.S. Ross, P.J. Stephens, V.A. Miller, S.M. Ali, C.M. Lovly

Acquisition of data (provided animals, acquired and managed patients, provided facilities, etc.): K. Konduri, J.-N. Gallant, F.J. Giles, E. Ichihara, T.K. Owonikoko, V. Peddareddigari, S.S. Ramalingam, S.K. Reddy, B. Eaby-Sandy, T. Vavalà, Y. Yan, J.S. Ross, S.M. Ali, C.M. Lovly

Analysis and interpretation of data (e.g., statistical analysis, biostatistics, computational analysis): J.-N. Gallant, F.J. Giles, K. Gowen, T.K. Owonikoko, V. Peddareddigari, S.S. Ramalingam, H. Chen, J.H. Sheehan, J. Meiler, J.S. Ross, S.M. Ali, C.M. Lovly

Writing, review, and/or revision of the manuscript: K. Konduri, J.-N. Gallant, Y.K. Chae, F.J. Giles, B.J. Gitlitz, K. Gowen, E. Ichihara, T.K. Owonikoko, V. Peddareddigari, S.S. Ramalingam, B. Eaby-Sandy, T. Vavalà, A. Whiteley, Y. Yan, J.H. Sheehan, J. Meiler, D. Morosini, J.S. Ross, P.J. Stephens, V.A. Miller, S.M. Ali, C.M. Lovly

Administrative, technical, or material support (i.e., reporting or organizing data, constructing databases): K. Konduri, Y.K. Chae, Y. Yan, J.S. Ross, S.M. Ali, C.M. Lovly

Study supervision: Y.K. Chae, F.J. Giles, V. Peddareddigari, J. Meiler, J.S. Ross, S.M. Ali, C.M. Lovly

Other (developed all hypotheses, designed all experiments, acquired most preclinical data, analyzed all data, created all figures, and wrote the manuscript): J.-N. Gallant

Other (contributed patients in manuscript): B.J. Gitlitz

Acknowledgments

The authors thank the patients and their families. They are grateful to William Pao and Catherine Meador for critical review of the manuscript.

Grant Support

This study was supported in part by the NIH and NCI R01CA121210 (C.M. Lovly) and P01CA129243. Research was supported by the 2015 AACR–Genentech BioOncology Career Development Award for Cancer Research on the HER Family Pathway, grant number 15-20-18-LOVL (to C.M. Lovly). C.M. Lovly, J.-N. Gallant, and J.H. Sheehan were supported by a V Foundation Scholar-in-Training Award. C.M. Lovly was additionally supported by a Damon Runyon Clinical Investigator Award and a LUNGevity Career Development Award. J.-N. Gallant was additionally supported by F30CA206339 and MSTP grant T32GM007347. Work in the Meiler laboratory is supported through the NIH (R01GM080403, R01GM099842, R01DK097376, R01HL122010, and R01GM073151) and the NSF (CHE1305874). T. Vavalà and B.J. Gitlitz were part of the Genomic of Young Lung Cancer study (GoYLC; NCT02273336), which was funded by the Bonnie J. Addario Lung Cancer Foundation, the Peter Barker Foundation, Genentech, the Beth Longwell Foundation, the Schmidt Legacy Foundation, and Upstage Lung Cancer.

Received January 16, 2016; revised April 13, 2016; accepted April 13, 2016; published OnlineFirst April 21, 2016.

REFERENCES

1. Lynch TJ, Bell DW, Sordella R, Gurubhagavatula S, Okimoto RA, Brannigan BW, et al. Activating mutations in the epidermal growth factor receptor underlying responsiveness of non-small-cell lung cancer to gefitinib. N Engl J Med 2004;350:2129–39.
2. Pao W, Miller V, Zakowski M, Doherty J, Politi K, Sarkaria I, et al. EGF receptor gene mutations are common in lung cancers from "never smokers" and are associated with sensitivity of tumors to gefitinib and erlotinib. Proc Natl Acad Sci U S A 2004;101:13306–11.
3. Paez JG, Jänne PA, Lee JC, Tracy S, Greulich H, Gabriel S, et al. EGFR mutations in lung cancer: correlation with clinical response to gefitinib therapy. Science 2004;304:1497–500.
4. Mok TS, Wu Y-L, Thongprasert S, Yang C-H, Chu D-T, Saijo N, et al. Gefitinib or carboplatin-paclitaxel in pulmonary adenocarcinoma. N Engl J Med 2009;361:947–57.
5. Rosell R, Carcereny E, Gervais R, Vergnenegre A, Massuti B, Felip E, et al. Erlotinib versus standard chemotherapy as first-line treatment for European patients with advanced EGFR mutation-positive non-small-cell lung cancer (EURTAC): a multicentre, open-label, randomised phase 3 trial. Lancet Oncol 2012;13:239–46.
6. Sequist LV, Yang JC-H, Yamamoto N, O'Byrne K, Hirsh V, Mok T, et al. Phase III study of afatinib or cisplatin plus pemetrexed in patients with metastatic lung adenocarcinoma with EGFR mutations. J Clin Oncol 2013;31:3327–34.
7. Gallant J-N, Sheehan JH, Shaver TM, Bailey M, Lipson D, Chandramohan R, et al. EGFR kinase domain duplication (EGFR-KDD) is a novel oncogenic driver in lung cancer that is clinically responsive to afatinib. Cancer Discov 2015;5:1155–63.
8. Baik CS, Wu D, Smith C, Martins RG, Pritchard CC. Durable response to tyrosine kinase inhibitor therapy in a lung cancer patient harboring epidermal growth factor receptor tandem kinase domain duplication. J Thorac Oncol 2015;10:e97–9.

Published OnlineFirst April 21, 2016; DOI: 10.1158/2159-8290.CD-16-0075

9. Frampton GM, Fichtenholtz A, Otto GA, Wang K, Downing SR, He J, et al. Development and validation of a clinical cancer genomic profiling test based on massively parallel DNA sequencing. Nat Biotechnol 2013;31:1023–31.
10. Eisenhauer EA, Therasse P, Bogaerts J, Schwartz LH, Sargent D, Ford R, et al. New response evaluation criteria in solid tumours: revised RECIST guideline (version 1.1). Eur J Cancer 2009;45:228–47.
11. Daley GQ, Baltimore D. Transformation of an interleukin 3-dependent hematopoietic cell line by the chronic myelogenous leukemia-specific P210bcr/abl protein. Proc Natl Acad Sci U S A 1988;85:9312–6.
12. Pruss RM, Herschman HR. Variants of 3T3 cells lacking mitogenic response to epidermal growth factor. Proc Natl Acad Sci U S A 1977;74:3918–21.
13. Jorissen RN, Walker F, Pouliot N, Garrett TPJ, Ward CW, Burgess AW. Epidermal growth factor receptor: mechanisms of activation and signalling. Exp Cell Res 2003;284:31–53.
14. Chung BM, Dimri M, George M, Reddi AL, Chen G, Band V, et al. The role of cooperativity with Src in oncogenic transformation mediated by non-small cell lung cancer-associated EGF receptor mutants. Oncogene 2009;28:1821–32.
15. Zhang X, Gureasko J, Shen K, Cole PA, Kuriyan J. An allosteric mechanism for activation of the kinase domain of epidermal growth factor receptor. Cell 2006;125:1137–49.
16. Shaw AT, Hsu PP, Awad MM, Engelman JA. Tyrosine kinase gene rearrangements in epithelial malignancies. Nat Rev Cancer 2013;13:772–87.
17. Conway AB, Lynch TW, Zhang Y, Fortin GS, Fung CW, Symington LS, et al. Crystal structure of a Rad51 filament. Nat Struct Mol Biol 2004;11:791–6.
18. Li S, Schmitz KR, Jeffrey PD, Wiltzius JJW, Kussie P, Ferguson KM. Structural basis for inhibition of the epidermal growth factor receptor by cetuximab. Cancer Cell 2005;7:301–11.
19. Stransky N, Cerami E, Schalm S, Kim JL, Lengauer C. The landscape of kinase fusions in cancer. Nat Commun 2014;5:1–10.
20. Vivanco I, Robins HI, Rohle D, Campos C, Grommes C, Nghiemphu PL, et al. Differential sensitivity of glioma- versus lung cancer-specific EGFR mutations to EGFR kinase inhibitors. Cancer Discov 2012;2:458–71.
21. Pirker R, Pereira JR, Szczesna A, von Pawel J, Krzakowski M, Ramlau R, et al. Cetuximab plus chemotherapy in patients with advanced non-small-cell lung cancer (FLEX): an open-label randomised phase III trial. Lancet 2009;373:1525–31.
22. Kim ES, Neubauer M, Cohn A, Schwartzberg L, Garbo L, Caton J, et al. Docetaxel or pemetrexed with or without cetuximab in recurrent or progressive non-small-cell lung cancer after platinum-based therapy: a phase 3, open-label, randomised trial. Lancet Oncol 2013;14:1326–36.
23. Cho J, Chen L, Sangji N, Okabe T, Yonesaka K, Francis JM, et al. Cetuximab response of lung cancer-derived EGF receptor mutants is associated with asymmetric dimerization. Cancer Res 2013;73:6770–9.
24. Brennan CW, Verhaak RGW, McKenna A, Campos B, Noushmehr H, Salama SR, et al. The somatic genomic landscape of glioblastoma. Cell 2013;155:462–77.
25. Cho J, Pastorino S, Zeng Q, Xu X, Johnson W, Vandenberg S, et al. Glioblastoma-derived epidermal growth factor receptor carboxyl-terminal deletion mutants are transforming and are sensitive to EGFR-directed therapies. Cancer Res 2011;71:7587–96.
26. Imielinski M, Berger AH, Hammerman PS, Hernandez B, Pugh TJ, Hodis E, et al. Mapping the hallmarks of lung adenocarcinoma with massively parallel sequencing. Cell 2012;150:1107–20.
27. Soda M, Choi YL, Enomoto M, Takada S, Yamashita Y, Ishikawa S, et al. Identification of the transforming EML4–ALK fusion gene in non-small-cell lung cancer. Nature 2007;448:561–6.
28. Rumora AE, Steere AN, Ramsey JE, Knapp AM, Ballif BA, Kelm RJ. Isolation and characterization of the core single-stranded DNA-binding domain of purine-rich element binding protein B (Purβ). Biochem Biophys Res Commun 2010;400:340–5.
29. Eswar N, Eramian D, Webb B, Shen M-Y, Sali A. Protein structure modeling with MODELLER. Methods Mol Biol 2008;426:145–59.
30. Simons KT, Kooperberg C, Huang E, Baker D. Assembly of protein tertiary structures from fragments with similar local sequences using simulated annealing and Bayesian scoring functions. J Mol Biol 1997;268:209–25.

Published OnlineFirst April 21, 2016; DOI: 10.1158/2159-8290.CD-16-0075

AACR American Association for Cancer Research

CANCER DISCOVERY

EGFR Fusions as Novel Therapeutic Targets in Lung Cancer

Kartik Konduri, Jean-Nicolas Gallant, Young Kwang Chae, et al.

Cancer Discov 2016;6:601-611. Published OnlineFirst April 21, 2016.